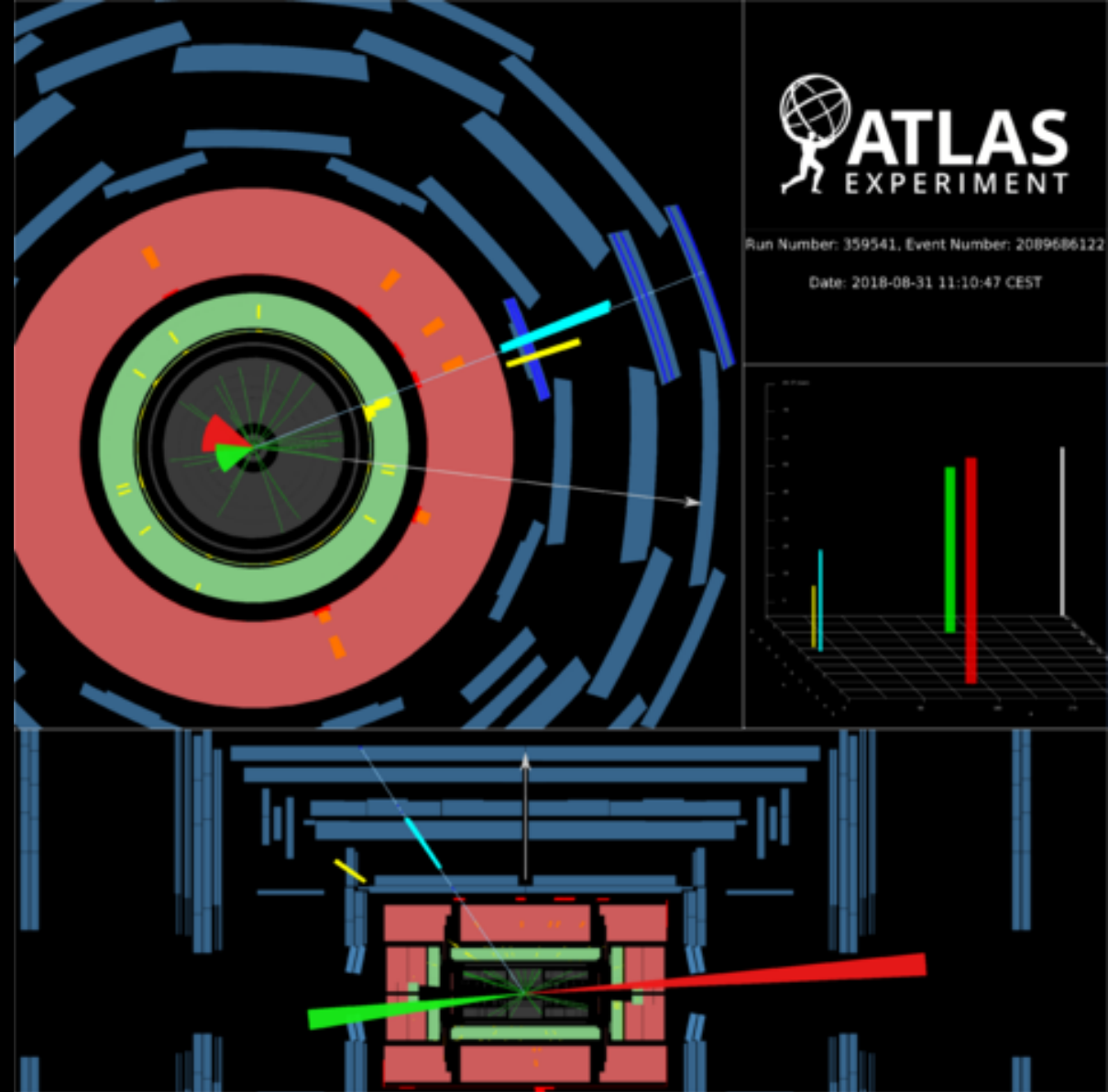


Measurements of gluon fusion and vector-boson-fusion production of the Higgs boson in  $H \rightarrow WW^* \rightarrow e\nu\mu\nu$  decays using 13 TeV  $pp$  collisions with the ATLAS detector

Robin Hayes

Higgs Hunting 2021



# Analysis Overview

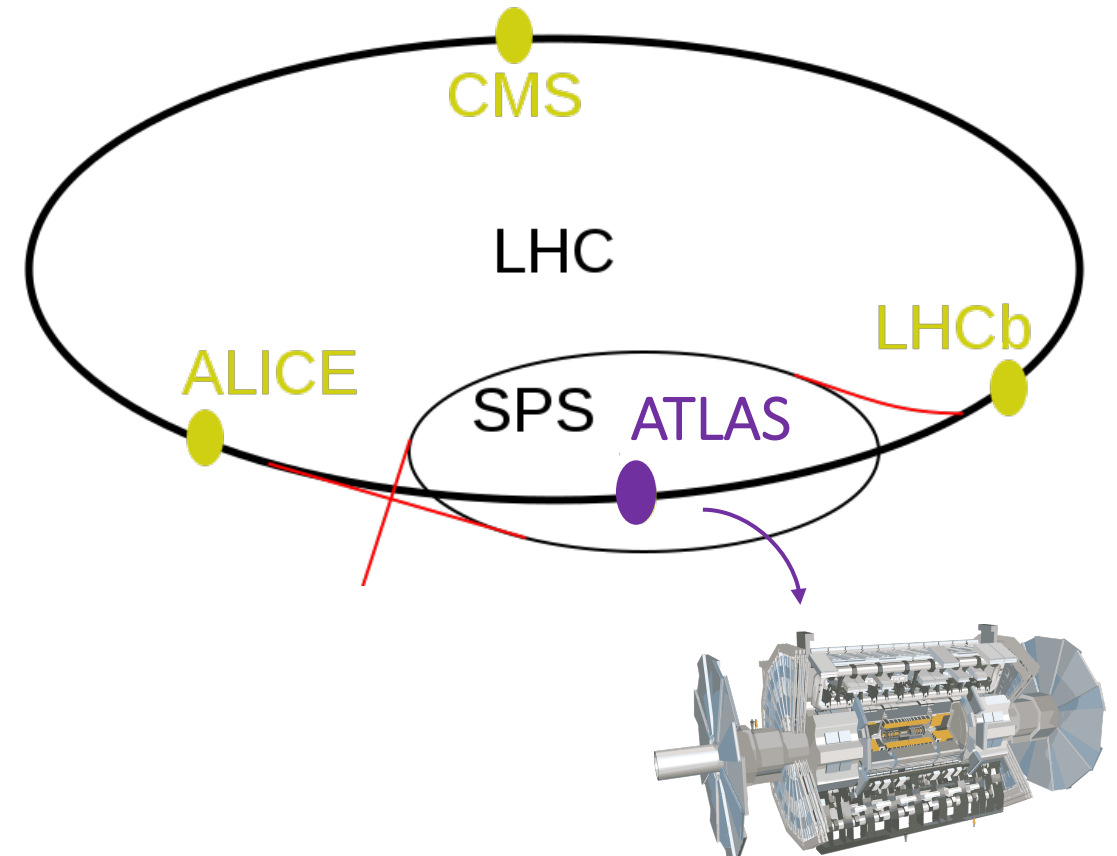
## Analysis Scope: [ATLAS-CONF-2021-014](#)

- ggF and VBF production of Higgs bosons in the  $H \rightarrow WW^* \rightarrow e\nu\mu\nu$  decay channel.
- Aim to measure cross-sections times branching fractions ( $\sigma^{\text{obs}} \cdot BR_{H \rightarrow WW^*}$ ) and signal strengths ( $\mu = \sigma^{\text{obs}} / \sigma^{\text{SM}}$ )

## Full Run-2 Result

- Data for this result comes from  $pp$  collisions at  $\sqrt{s} = 13$  TeV at CERN's Large Hadron Collider (LHC).
  - Collected between 2015-2018 ("Run 2") with the [ATLAS detector](#).
- This analysis makes several changes with respect to the previous ( $36 \text{ fb}^{-1}$ ) ATLAS measurement [1]:
  - ✓ Addition of ggF  $\geq 2$ -jet channel
  - ✓ Use of deep neural network (DNN) in VBF channel
  - ✓ Measurement of cross-sections in kinematic bins ("STXS").

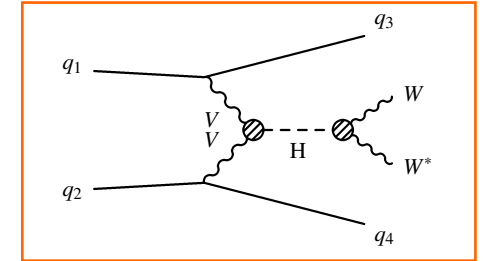
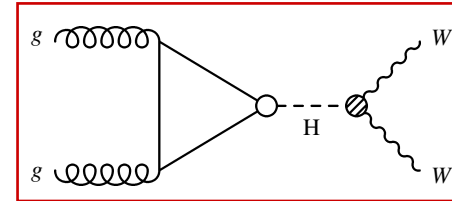
1. [arXiv: 1808.09054 \[hep-ex\]](#)



# Analysis Strategy

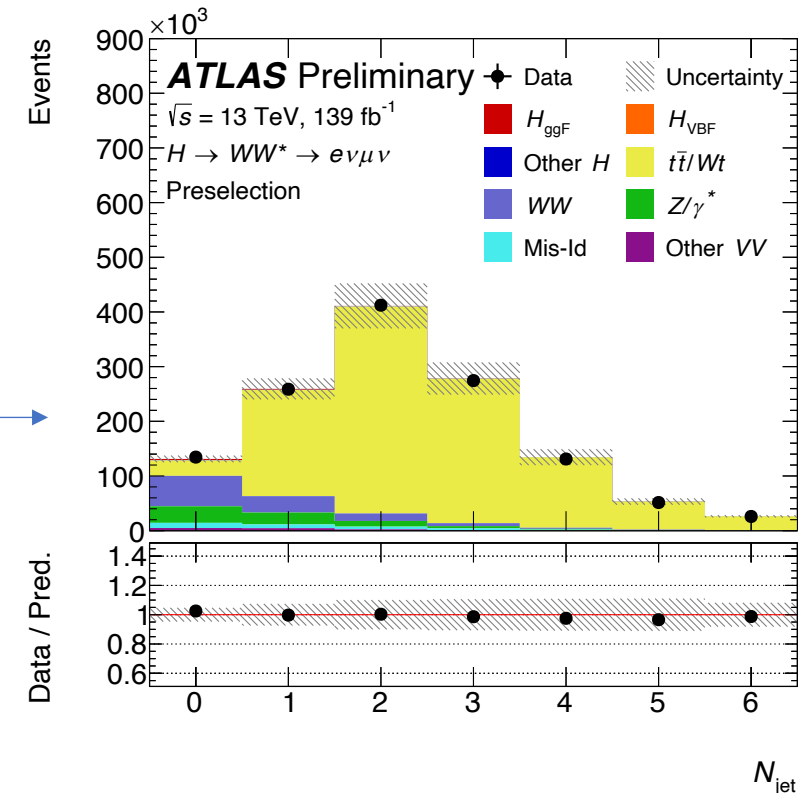
## Common Preselection:

- Cuts target features of  $H \rightarrow WW^* \rightarrow e\nu\mu\nu$  decay and reduce some common backgrounds:
  - ✓ Single-lepton and dilepton triggers used
  - ✓ 2 different-flavour, opposite-charge leptons
  - ✓  $p_T^{\text{lead}} > 22 \text{ GeV}$ ,  $p_T^{\text{sublead}} > 15 \text{ GeV}$
  - ✓  $m_{ll} > 10 \text{ GeV}$
  - ✓  $p_T^{\text{miss}} > 20 \text{ GeV}$  (ggF channels only)



## Defining Analysis Channels:

- Channels split by number of jets with  $p_T > 30 \text{ GeV}$  after preselection:
  - $N_{\text{jets}} = 0$  and  $N_{\text{jets}} = 1$  channels to target **ggF**
  - $N_{\text{jets}} \geq 2$  channels to target **ggF** and **VBF**
- Motivated by differing background compositions in each region.
- Remaining cuts are targeted to each analysis category.



# ggF 0-jet and 1-jet Channels

## Background rejection

$$\checkmark N_{b\text{-jet}}^{p_T > 20 \text{ GeV}} = 0 \quad \left. \vphantom{N_{b\text{-jet}}^{p_T > 20 \text{ GeV}}} \right\} \text{0 \& 1-jet}$$

$$\checkmark \Delta\phi_{ll, E_T^{\text{miss}}} > \pi/2$$

$$\checkmark p_T^l > 30 \text{ GeV}$$

0-jet

$$\checkmark m_{\tau\tau} < m_Z - 25 \text{ GeV}$$

$$\checkmark \max(m_T^l) > 50 \text{ GeV}$$

1-jet

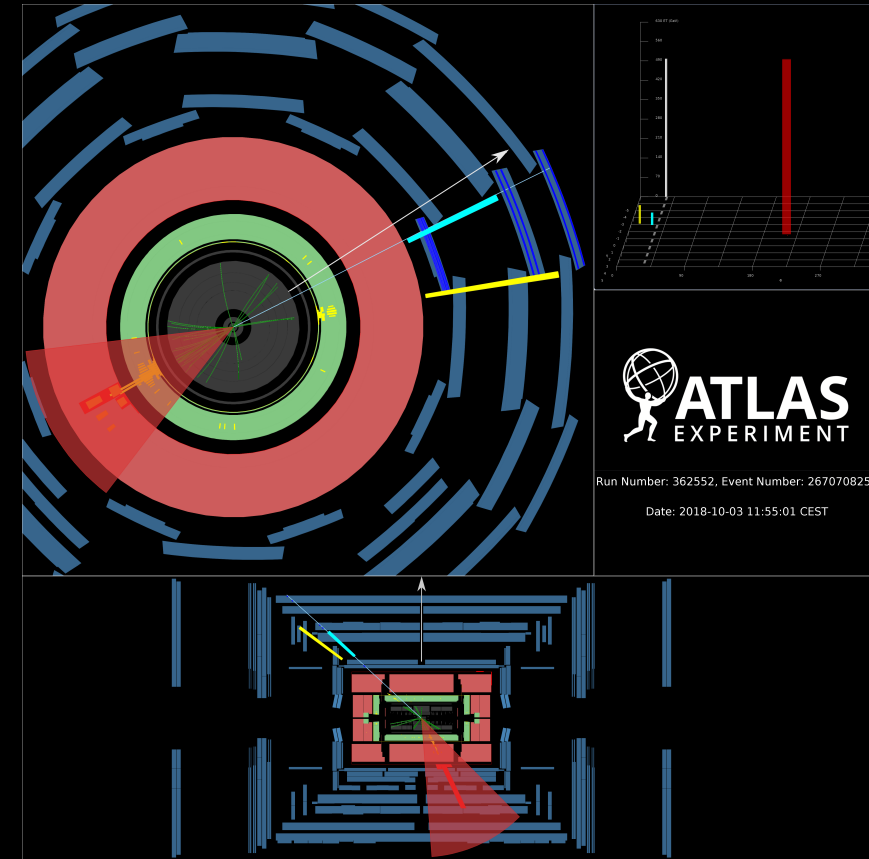
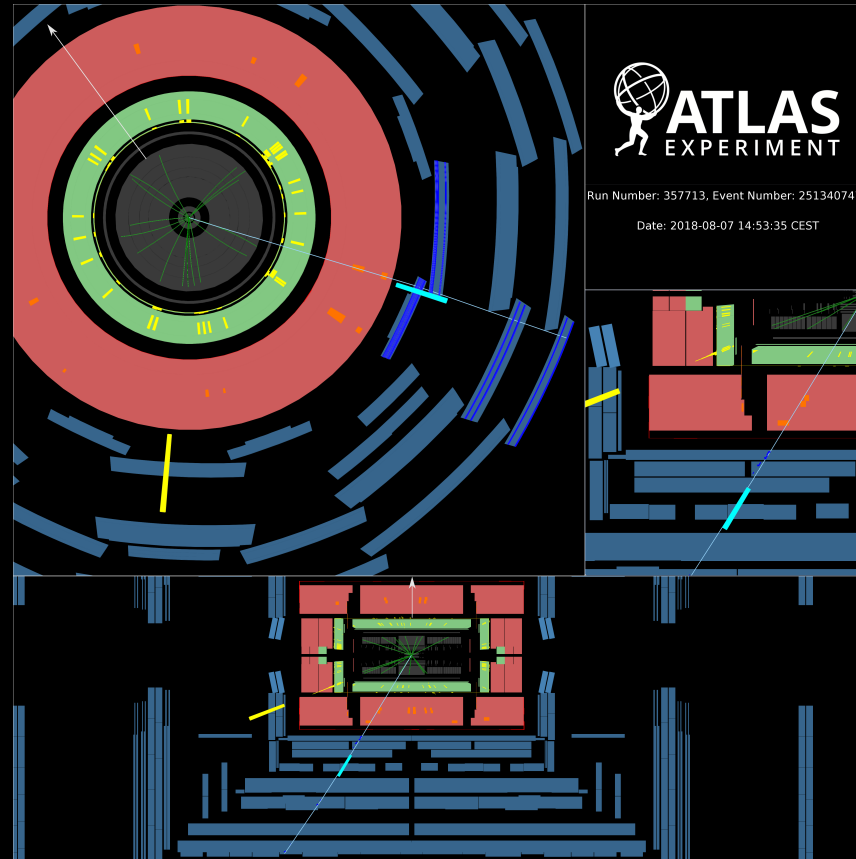
$H \rightarrow WW^* \rightarrow e\nu\mu\nu$   
topology

$$\checkmark m_{ll} < 55 \text{ GeV}$$

$$\checkmark \Delta\phi_{ll} < 1.8$$

Control regions for  
top,  $qqWW$ ,  $Z/\gamma^*$   
backgrounds.

Four signal regions each,  
split at  $m_{ll} = 30 \text{ GeV}$  and  
 $p_T^{\text{sublead}} = 20 \text{ GeV}$



# ggF $\geq 2$ -jet Channel

## Background rejection

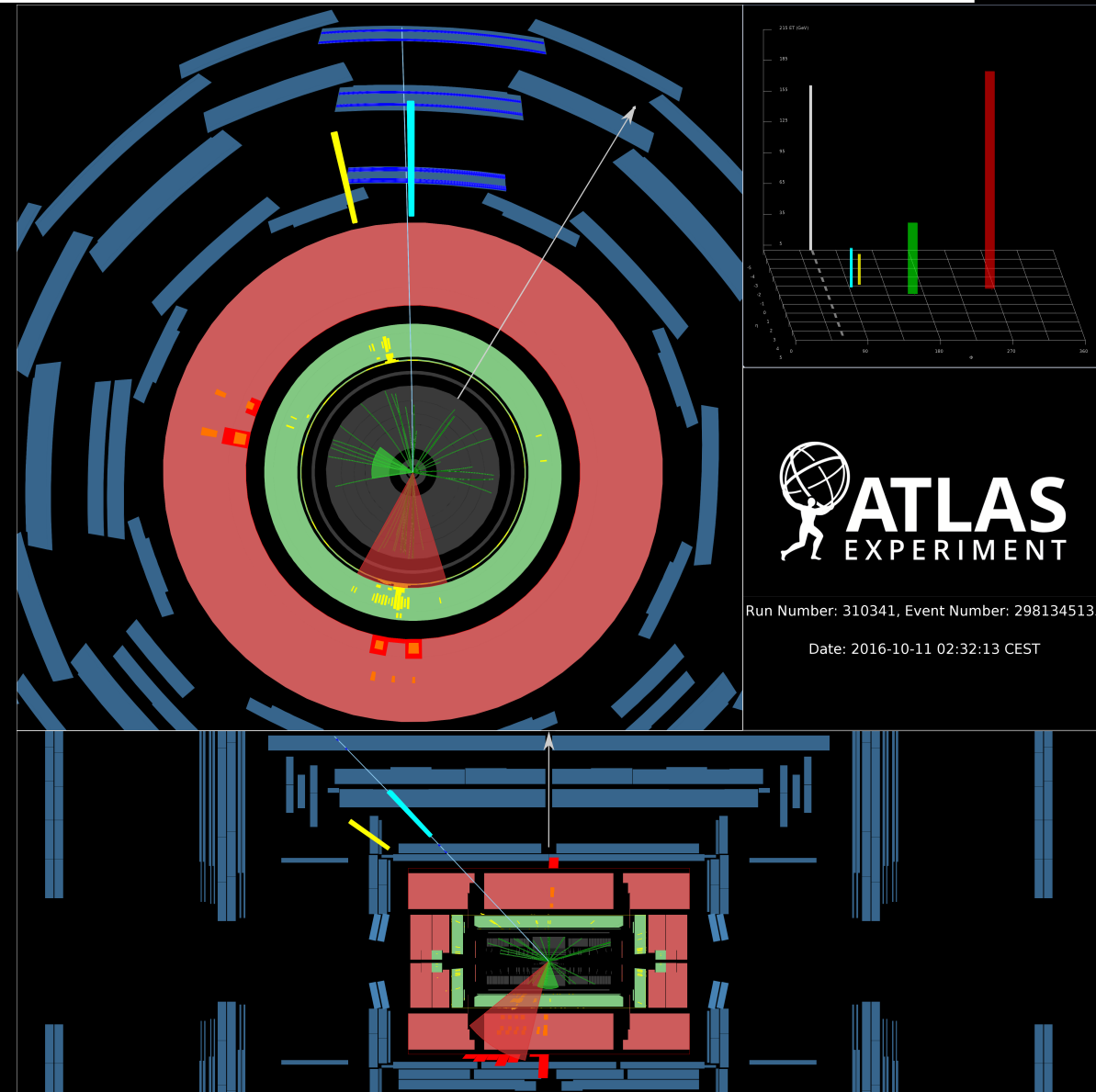
- ✓  $N_{b\text{-jet}}^{p_T > 20 \text{ GeV}} = 0$
- ✓  $m_{\tau\tau} < m_Z - 25 \text{ GeV}$

## $H \rightarrow WW^* \rightarrow e\nu\mu\nu$ topology

- ✓  $m_{ll} < 55 \text{ GeV}$
- ✓  $\Delta\phi_{ll} < 1.8$
- ✓  $|m_{jj} - 85| \leq 15 \text{ GeV}$  or  $\Delta y_{jj} > 1.2$
- ✓ Orthogonality with VBF analysis (fail central jet veto or outside lepton veto)

Control regions for top,  $qqWW$ ,  $Z/\gamma^*$  backgrounds.

Two signal regions split at  $m_{ll} = 30 \text{ GeV}$ .



# VBF $\geq 2$ -jet Channel

## Background rejection

- ✓  $N_{b\text{-jet}}^{p_T > 20 \text{ GeV}} = 0$
- ✓  $m_{\tau\tau} < m_Z - 25 \text{ GeV}$

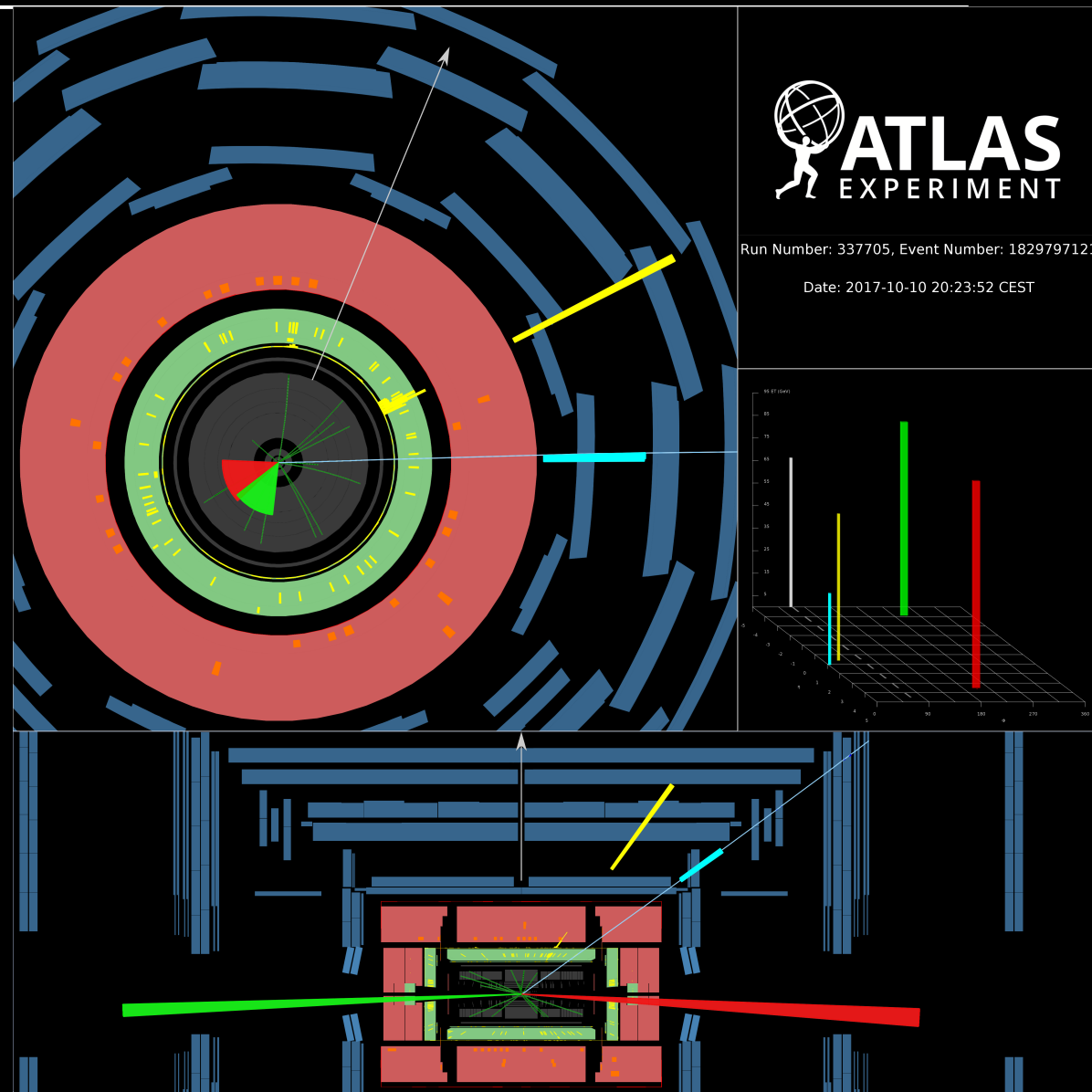
## $H \rightarrow WW^* \rightarrow e\nu\mu\nu$ topology

- ✓ Central jet veto
- ✓ Outside lepton veto
- ✓  $m_{jj} > 120 \text{ GeV}$  (Orthogonality with VH analysis)

Control regions for top,  $Z/\gamma^*$  backgrounds.

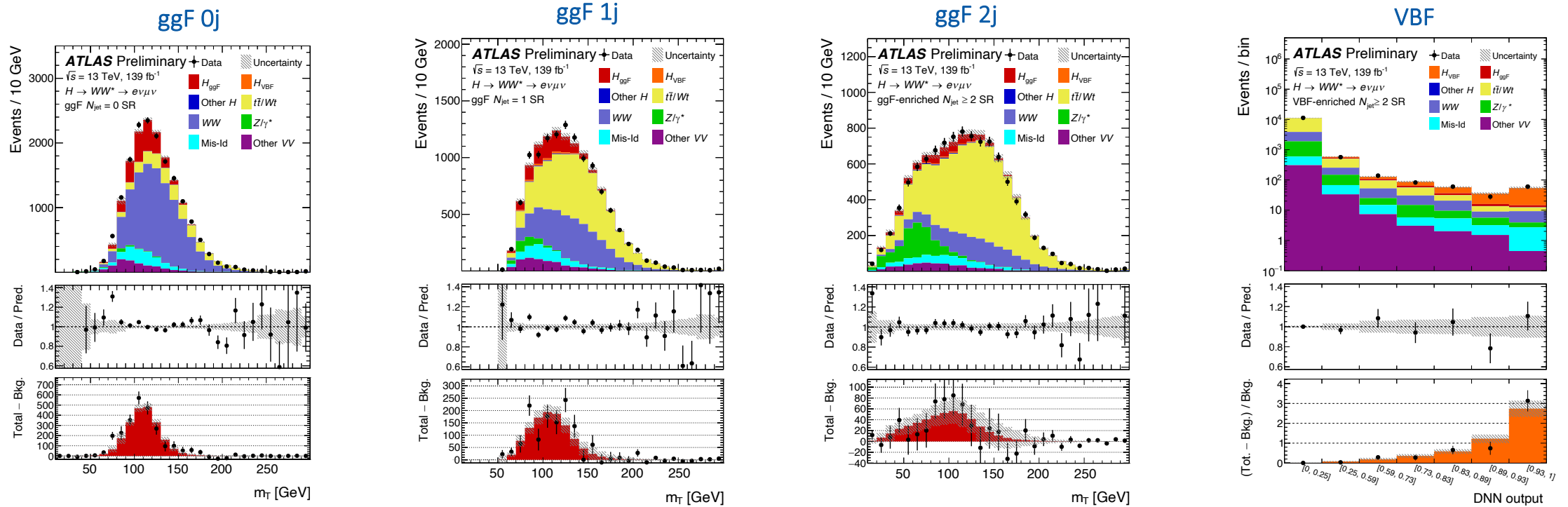
Events categorized by DNN score based on 15 variables:

$$\Delta y_{jj}, m_{jj}, \eta_\ell^{\text{centrality}}, m_{\ell_1 j_1}, m_{\ell_1 j_2}, m_{\ell_2 j_1}, m_{\ell_2 j_2}, \\ p_T^{\text{jet}_1}, p_T^{\text{jet}_2}, p_T^{\text{jet}_3}, \Delta\phi_{\ell\ell}, m_{\ell\ell}, m_T, p_T^{\text{tot}}, \text{MET sig}$$



# Results: Inclusive ggF and VBF Cross-Sections

- Final discriminant:  $m_T$  (ggF analyses) or DNN output (VBF analysis).
- Extract signal strengths using a **profile likelihood fit** to data in the signal and control regions.

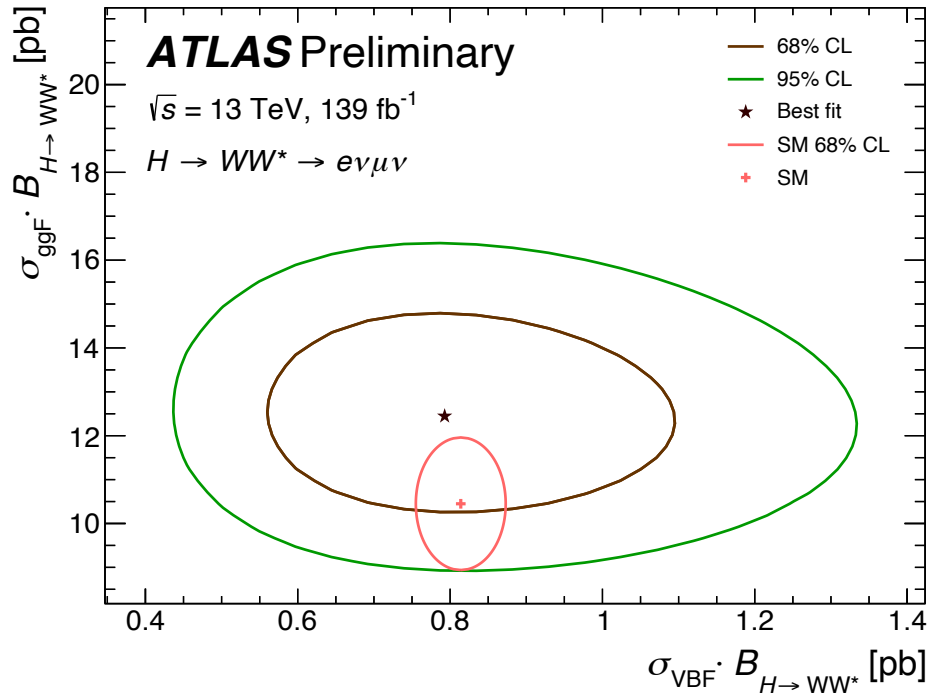


Simultaneous measurement of ggF and VBF **signal strengths** shows good consistency with the SM:

$\mu_{\text{ggF}} = 1.20^{+0.16}_{-0.15}$ $= 1.20 \pm 0.05 \text{ (stat.) }^{+0.09}_{-0.08} \text{ (exp syst.) }^{+0.10}_{-0.08} \text{ (sig theo.) }^{+0.12}_{-0.11} \text{ (bkg theo.)}$	$\mu_{\text{VBF}} = 0.99^{+0.24}_{-0.20}$ $= 0.99^{+0.13}_{-0.12} \text{ (stat.) }^{+0.07}_{-0.06} \text{ (exp syst.) }^{+0.17}_{-0.12} \text{ (sig theo.) }^{+0.10}_{-0.08} \text{ (bkg theo.)}$
--	---

# Results: Inclusive ggF and VBF Cross-Sections

Also measure cross-sections times branching fractions for both production modes:



$$\begin{aligned} \sigma_{\text{ggF}} \cdot \mathcal{B}_{H \rightarrow WW^*} &= 12.4 \pm 1.5 \text{ pb} \\ &= 12.4 \pm 0.6 \text{ (stat.)} \pm 0.9 \text{ (exp syst.)} {}^{+0.7}_{-0.6} \text{ (sig theo.)} \pm 1.0 \text{ (bkg theo.) pb} \\ \sigma_{\text{VBF}} \cdot \mathcal{B}_{H \rightarrow WW^*} &= 0.79 {}^{+0.19}_{-0.16} \text{ pb} \\ &= 0.79 {}^{+0.11}_{-0.10} \text{ (stat.)} {}^{+0.06}_{-0.05} \text{ (exp syst.)} {}^{+0.13}_{-0.09} \text{ (sig theo.)} {}^{+0.08}_{-0.06} \text{ (bkg theo.) pb,} \end{aligned}$$

Source	$\frac{\Delta\sigma_{\text{ggF}} \cdot \mathcal{B}_{H \rightarrow WW^*}}{\sigma_{\text{ggF}} \cdot \mathcal{B}_{H \rightarrow WW^*}}$ [%]	$\frac{\Delta\sigma_{\text{VBF}} \cdot \mathcal{B}_{H \rightarrow WW^*}}{\sigma_{\text{VBF}} \cdot \mathcal{B}_{H \rightarrow WW^*}}$ [%]
Data statistical uncertainties	5	13
Total systematic uncertainties	11	18
MC statistical uncertainties	4	3.2
Experimental uncertainties	6	7
Flavour Tagging	2.4	0.9
Jet energy scale	1.4	3.3
Jet energy resolution	2.3	1.9
$E_T^{\text{miss}}$	1.9	5
Muons	2.1	0.7
Electrons	1.5	0.3
Fake factors	2.4	1.0
Pile-up	2.4	1.3
Luminosity	2.0	2.1
<b>Theoretical uncertainties</b>	<b>8</b>	<b>16</b>
ggF	5	4
VBF	0.7	13
Top	4	5
$Z\tau\tau$	2.0	2.1
WW	4	5
Other $VV$	3	1.2
Background normalisations	5	5
WW	3.1	0.5
Top	2.4	2.2
$Z\tau\tau$	3.1	4
<b>TOTAL</b>	<b>12</b>	<b>22</b>

Largest contribution to measurement uncertainty comes from **theory uncertainty** on the **signal** (for  $\sigma_{\text{VBF}}$ ) and **background** (for  $\sigma_{\text{ggF}}$ ).

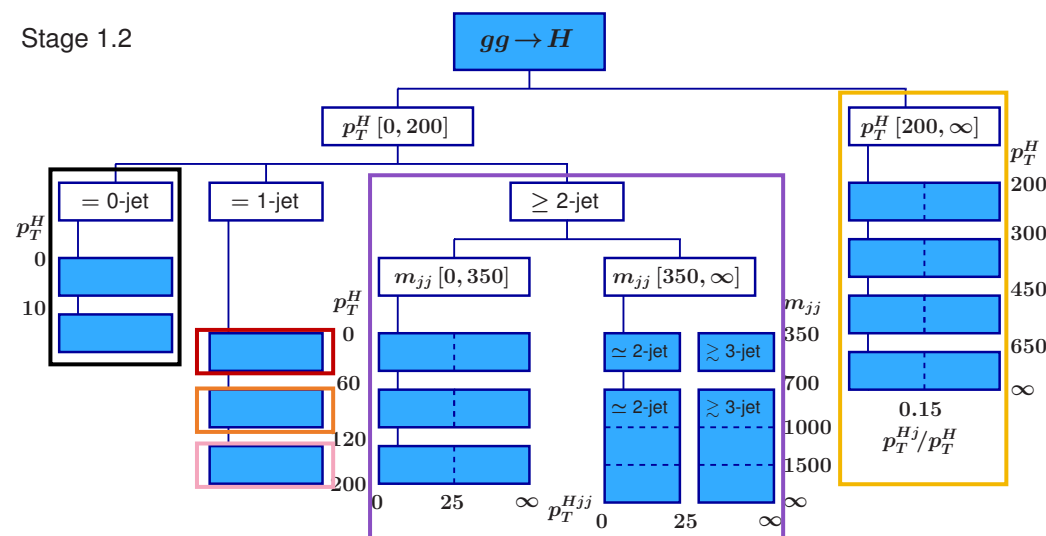


# Simplified Template Cross-Sections

- Results are extended with measurement of cross-sections in kinematic bins prescribed by the **Simplified Template Cross-Section (STXS) framework**.
- Cross-section measured are defined by STXS Stage 1.2 splitting, with bins merged according to analysis sensitivity.

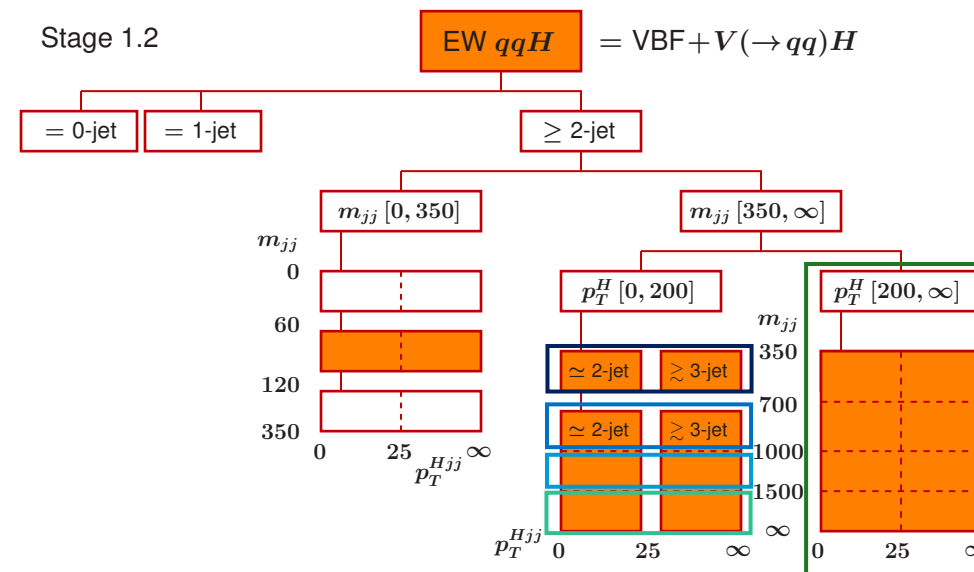
## ggH production:

- Measure 6 POIs
- Targeted by 0, 1 and  $\geq 2$ -jet ggF signal regions further split by  $p_T^H$ .



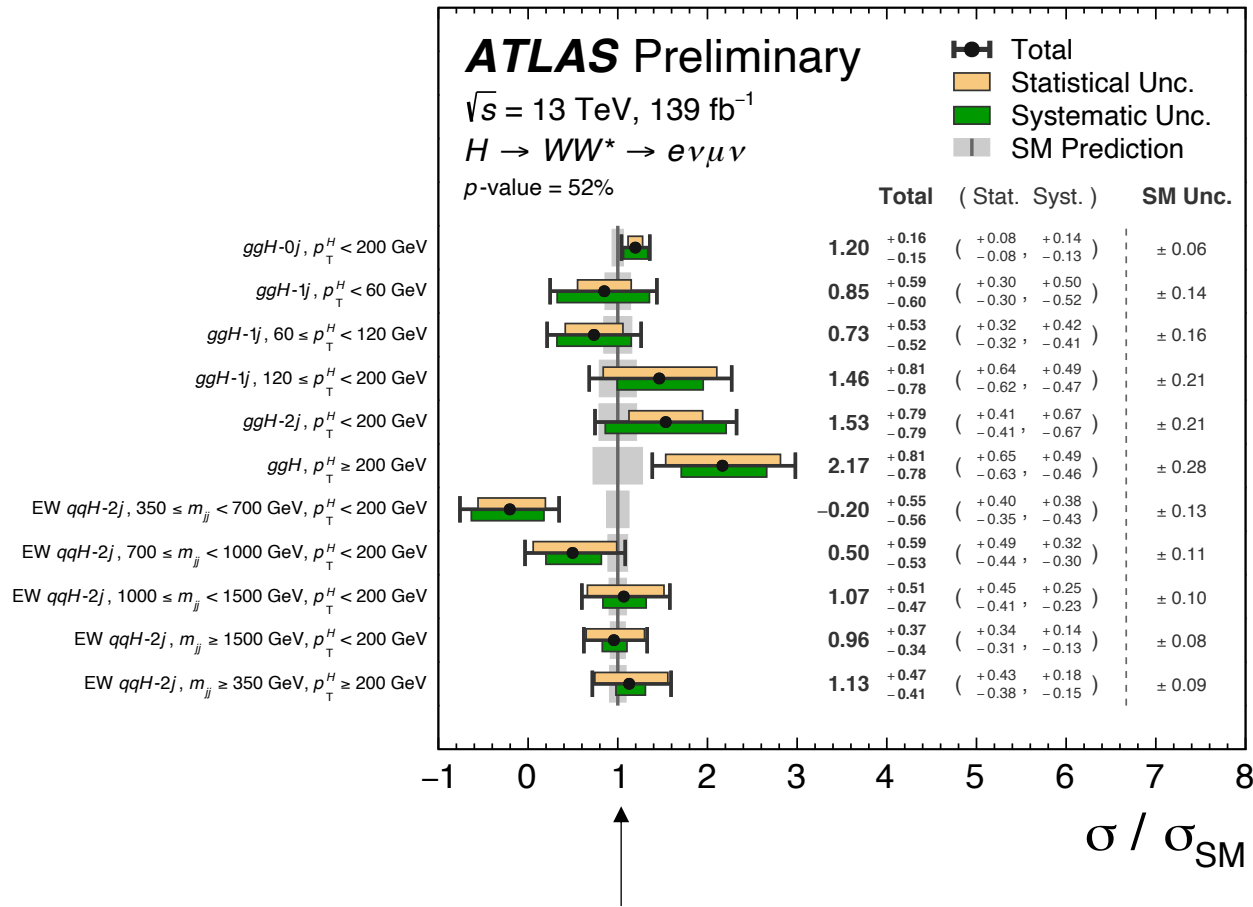
## EW qqH production:

- Measure 5 POIs
- Targeted by  $\geq 2$ -jet VBF signal region split by  $m_{jj}$ ,  $p_T^H$ .

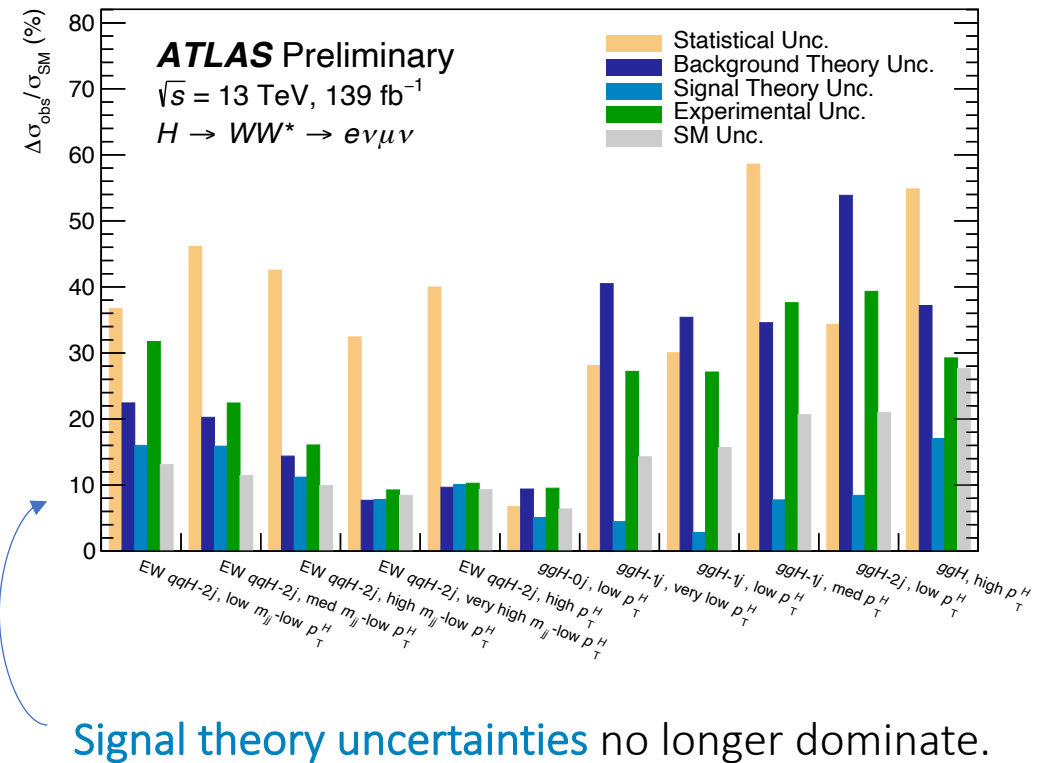


# Results: Simplified Template Cross-Sections

Ratio of measured cross-section to SM prediction shown for all 11 cross-sections:



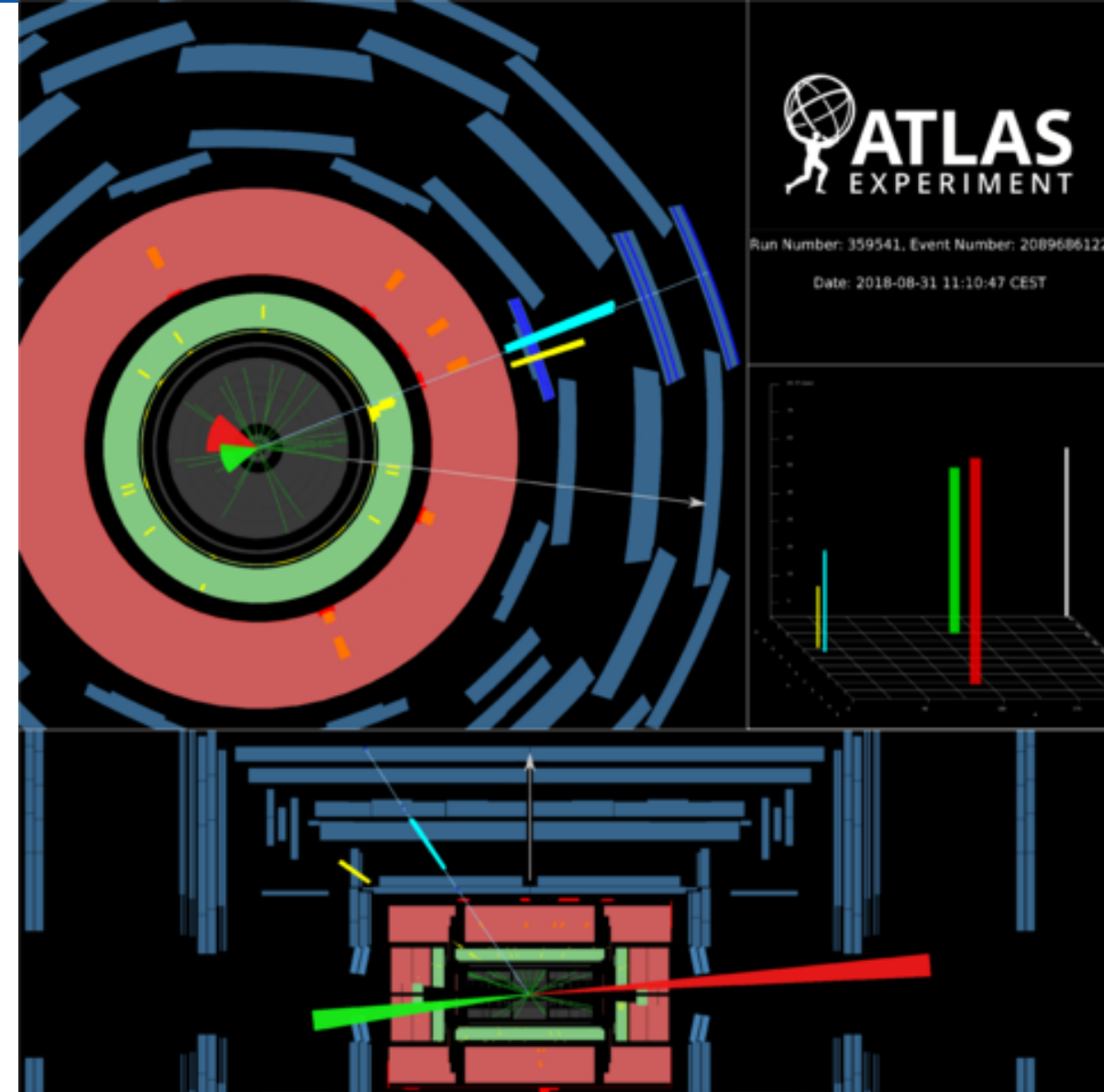
Results are compatible with the SM.



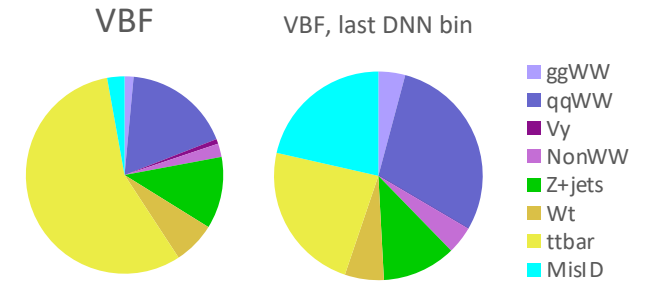
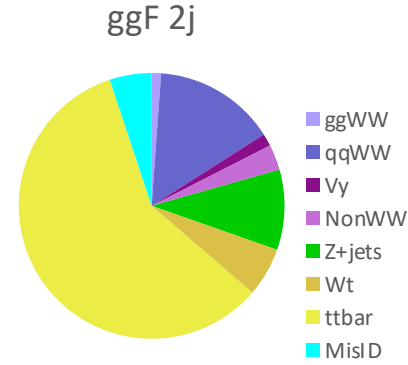
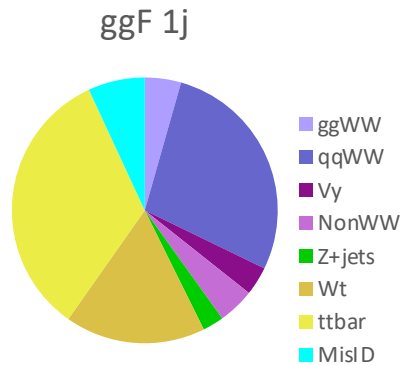
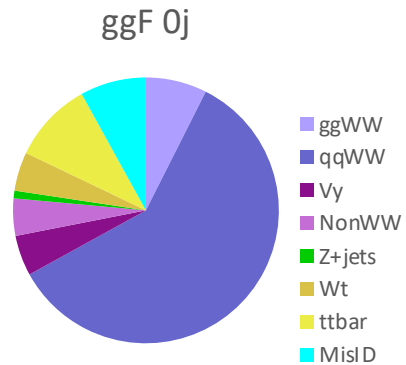
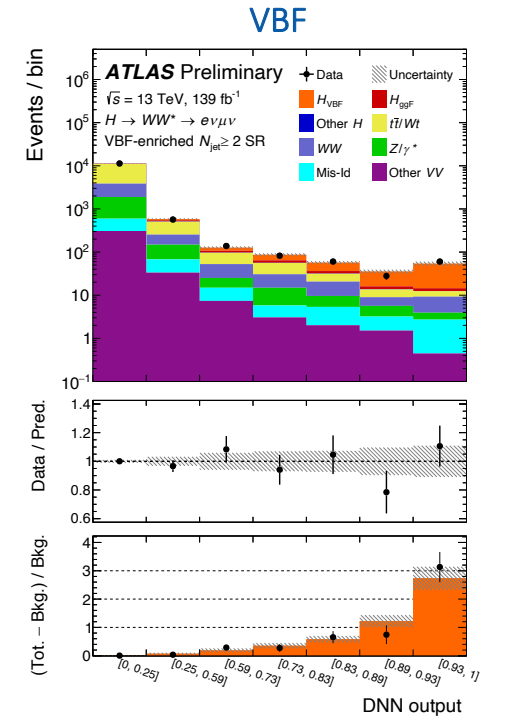
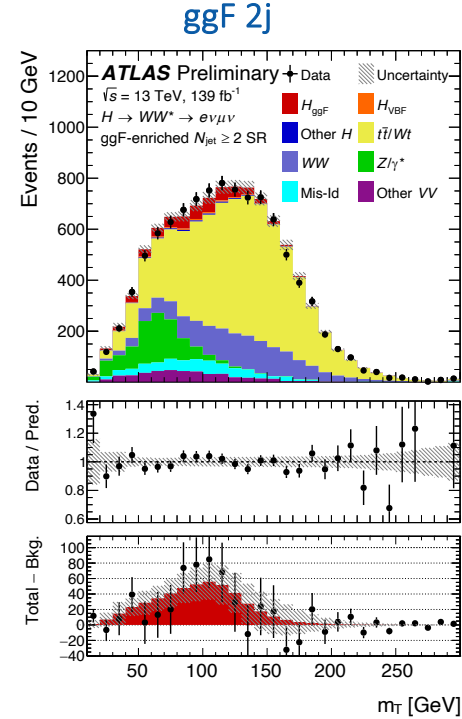
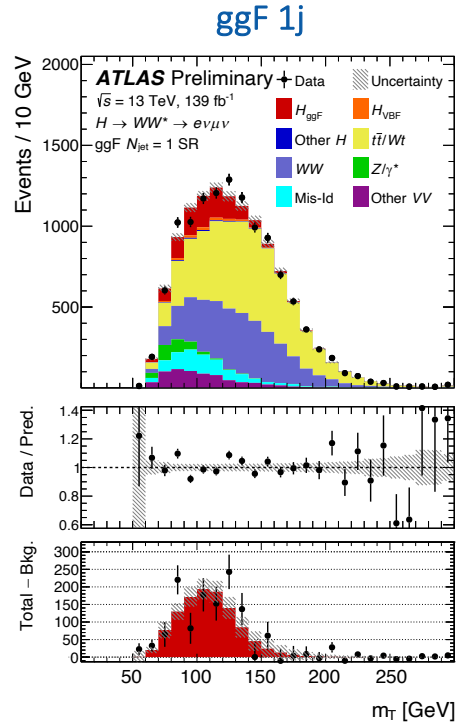
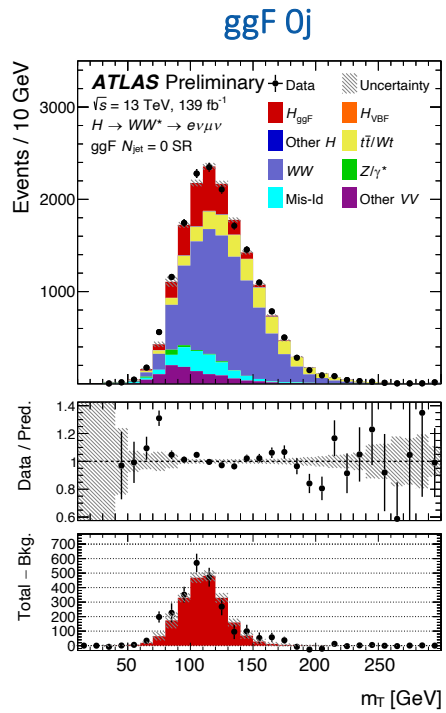
Most analysis categories are statistically-limited, with some ggH modes affected predominantly by background theory uncertainties.

# Conclusions

- This measurement of inclusive VBF and ggF  $H \rightarrow WW^*$  cross-sections is the most precise to-date, and so far shows consistency with the SM.
- Measurements in STXS bins also agree with the SM, and (for EW qqH) have a precision competitive with the latest combination of all Higgs results measured with the ATLAS detector [[ATLAS-CONF-2020-027](#)].
- Future measurements will benefit from a larger dataset and improving understanding of measurement uncertainties to further test the limits of the SM.

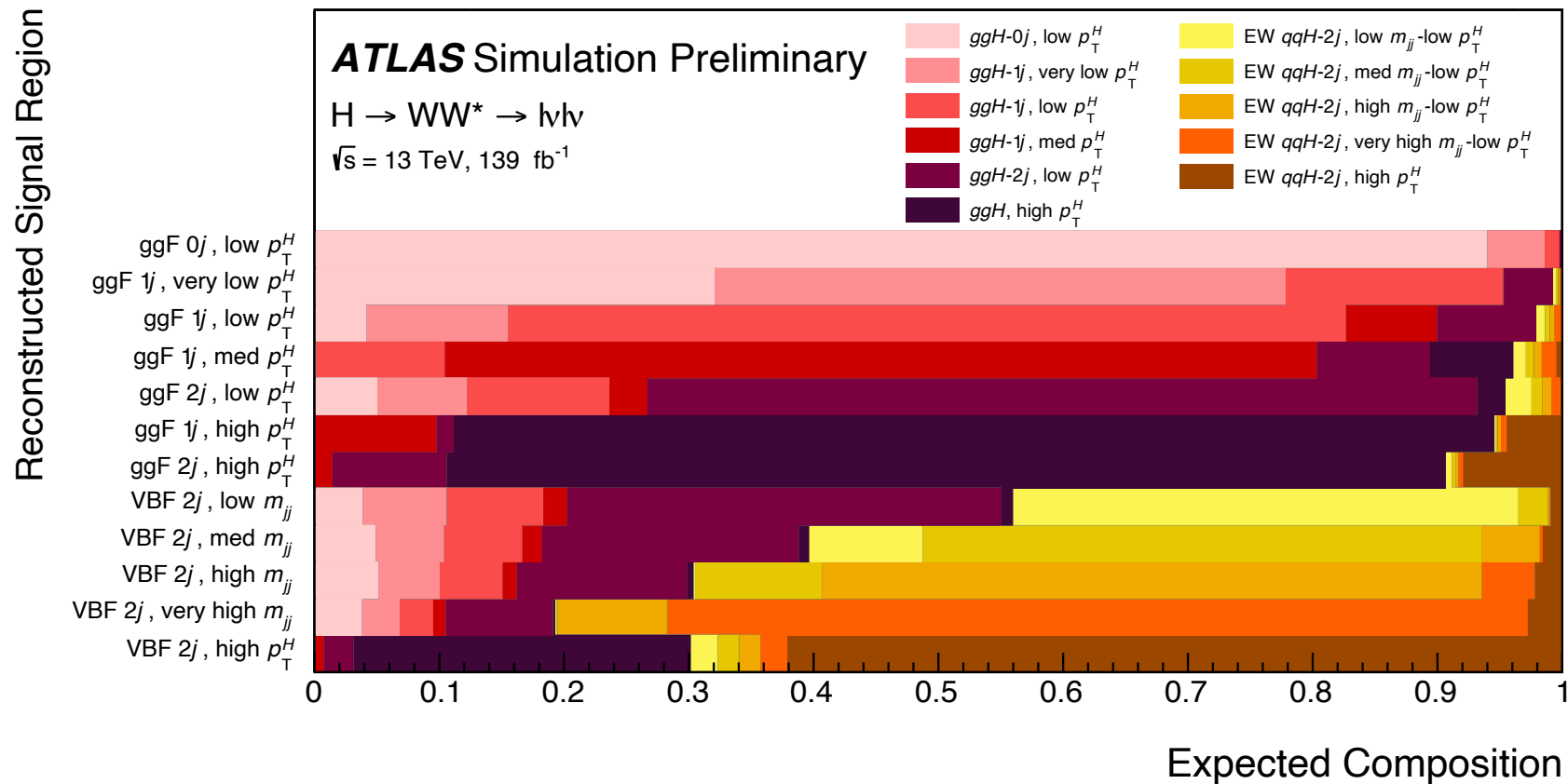


# Backgrounds

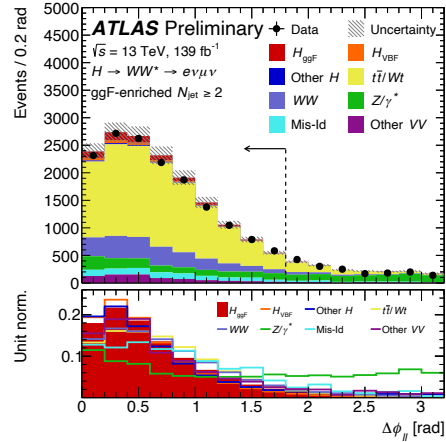


# Simplified Template Cross-Sections

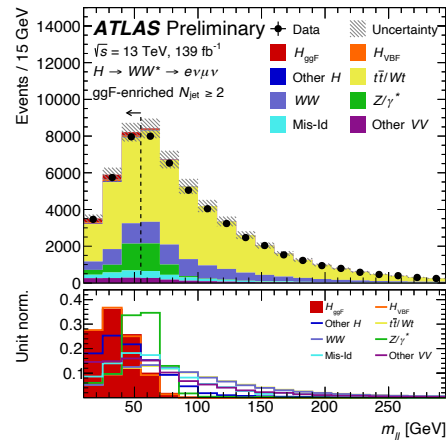
- ✓ Largest contribution to each reconstructed signal region come from the truth category it targets.



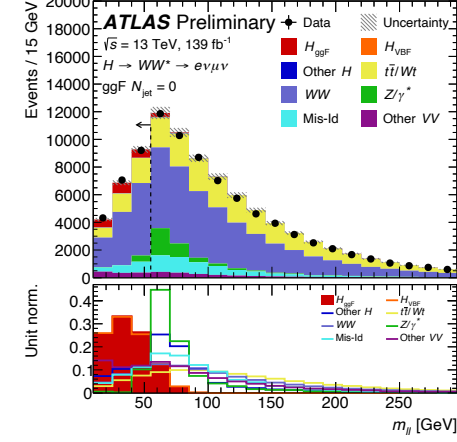
# Selections



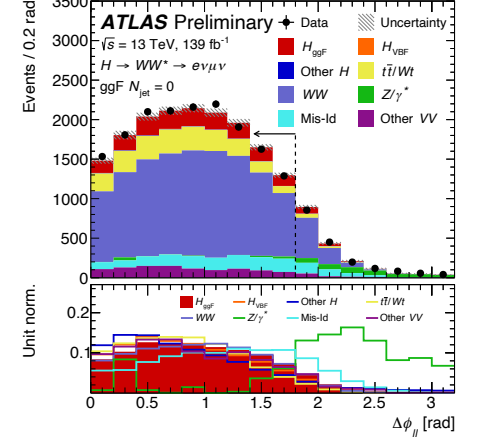
(a)



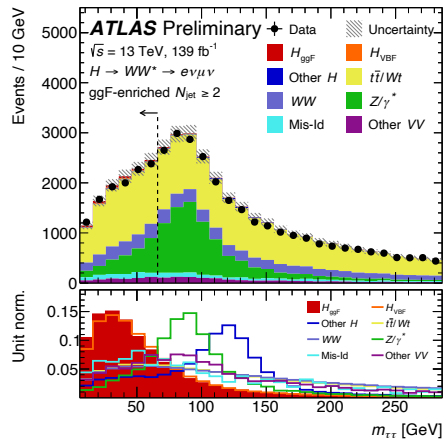
(b)



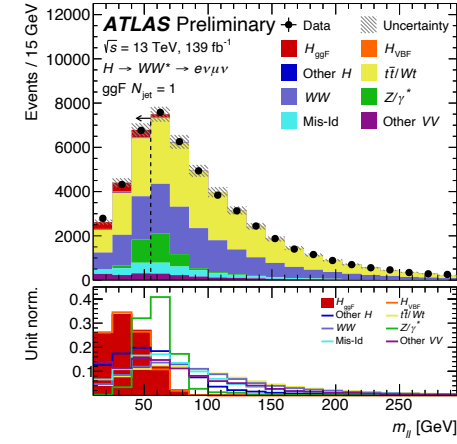
(a)



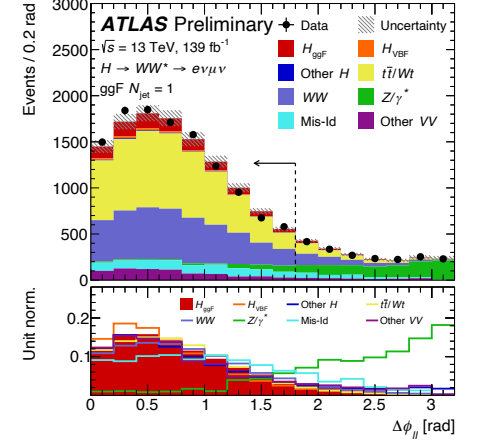
(b)



(c)



(c)

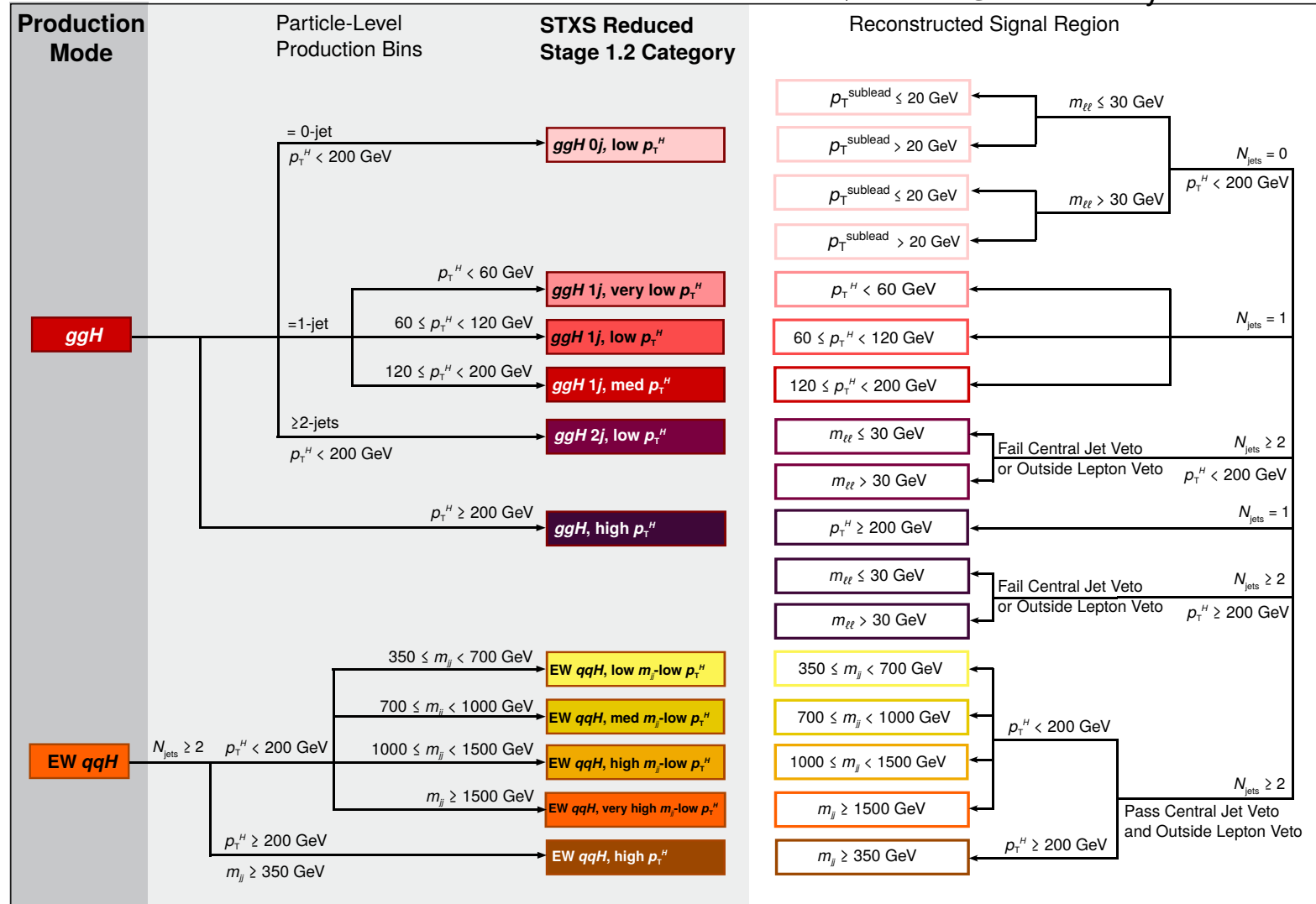


(d)

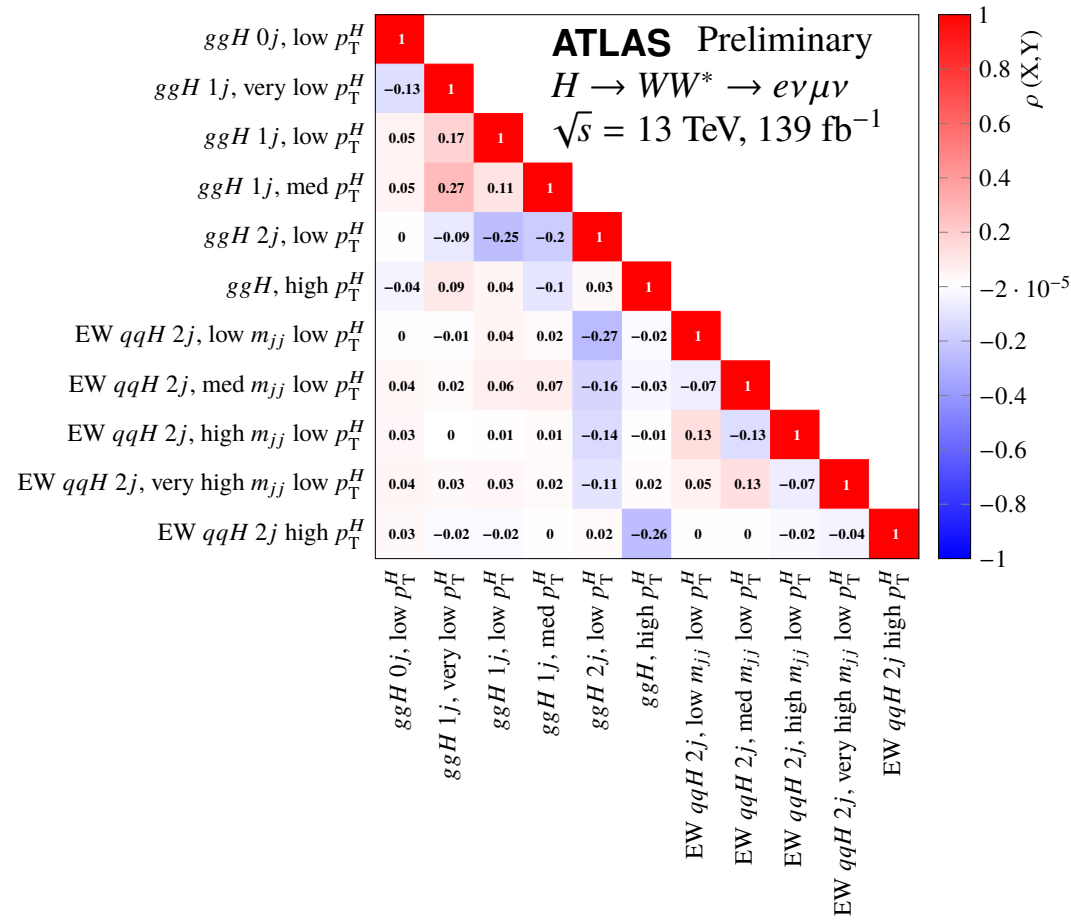
$$m_T = \sqrt{(E_T^{\ell\ell} + E_T^{\text{miss}})^2 - |\mathbf{p}_T^{\ell\ell} + \mathbf{E}_T^{\text{miss}}|^2}$$

# Selections

$H \rightarrow WW^* \rightarrow e\nu_e\mu\nu_\mu$  **ATLAS Preliminary**  $\sqrt{s} = 13$  TeV



# Results



Category	WW	$t\bar{t}/Wt$	$Z/\gamma^*$
$N_{\text{jet},(p_T>30 \text{ GeV})} = 0$ ggF	$1.03^{+0.07}_{-0.07}$	$0.96^{+0.23}_{-0.18}$	$0.96^{+0.07}_{-0.06}$
$N_{\text{jet},(p_T>30 \text{ GeV})} = 1$ ggF	$0.82^{+0.15}_{-0.14}$	$1.07^{+0.19}_{-0.16}$	$0.97^{+0.10}_{-0.09}$
$N_{\text{jet},(p_T>30 \text{ GeV})} \geq 2$ ggF	$0.80^{+0.35}_{-0.34}$	$0.94^{+0.23}_{-0.18}$	$0.97^{+0.18}_{-0.16}$
$N_{\text{jet},(p_T>30 \text{ GeV})} \geq 2$ VBF	–	$1.00^{+0.37}_{-0.22}$	$0.96^{+0.25}_{-0.20}$